APPLYING TWO METHODOLOGIES OF AN INTEGRATED COASTAL VULNERABILITY INDEX (ICVI) TO FUTURE SEA-LEVEL RISE. CASE STUDY: SOUTHERN COAST OF THE GULF OF CORINTH, GREECE

PRIMJENA DVIJE METODOLOGIJE INTEGRIRANOG INDEKSA RANJIVOSTI OBALNOG PODRUČJA (ICVI) NA BUDUĆI PORAST RAZINE MORA. STUDIJA SLUČAJA: JUŽNA OBALA KORINTSKOG ZALJEVA, GRČKA

PASCHALIS RAMNALIS,* DIMITRIOS-VASILEIOS BATZAKIS, EFTHIMIOS KARYMBALIS

Department of Geography, Harokopio University, Eleftheriou Venizelou Ave., 70, GR-176 76 Kallithea, Athens, Greece / *Odjel za geografiju, Sveučilište Harokopio, Atena, Grčka*, e-mail: geopas100@gmail.com, mpatzakis@hua.gr, karymbalis@hua.gr

* corresponding author / *autor za kontakt*

DOI: 10.15291/geoadria.4046
Original scientific paper / *Izvorni znanstveni rad*
Received / *Primljeno*: 3-12-2022
Accepted / *Prihvaćeno*: 19-2-2023

Climate change is an issue of concern and is expected to cause various adverse impacts on human societies in the near and long-term future. Sea-level rise, which is caused by global warming and melting continental ice sheets, in combination with the rising global population and evolution of human activities in coastal areas, tends to make coastal societies more prone to coastal hazards. The Gulf of Corinth in Greece with its diverse coastal landforms and tectonic complexity makes the region unique when considering an assessment of coastal vulnerability. In this study we apply an Integrated Coastal Vulnerability Index (ICVI) to a potential sea-level rise for the southern coastline of the Gulf of Corinth (Greece) consisting of physical and socio-economic parameters. Among multiple different methodologies that have been developed over the recent years, we decided to apply two of the mathematical approaches we believe are best suited for the protection of human activities in our study area. The first one, ICVI_1, is based on the Coastal Vulnerability Index (CVI) by Thieler and Hammar-Klose (1999) with variables of equal relative importance, whereas the second one, ICVI_2, uses the Analytic Hierarchic Process (AHP) with the assignment of relative weight values to each parameter. The parameters were identified and ranked into a vulnerability index with a scale from 1 to 5. The results reveal that both approaches depict more or less the same coastal sections of high or very high vulnerability, but differ in the distribution of extreme values. ICVI_1 shows that 18.3% of the total coastline features very high vulnerability (score 5), while ICVI_2 shows 9.1%. The coastal sections with the highest scores of vulnerability are mostly represented in the eastern part of the studied coastline with low-lying regions of gentle slope and concentrated human activity.

Key words: climate change, sea-level rise, coastal vulnerability, AHP,

Problem klimatskih promjena izaziva zabrinutost te se očekuje da će negativno utjecati na društvo u bliskoj i dugoročnoj budućnosti. Porast razine mora, uzrokovan globalnim zagrijavanjem i otapanjem kontinentalnih ledenih ploča, u kombinaciji s rastućom globalnom populacijom i razvojem ljudskih aktivnosti u obalnim područjima, čini obalna društva sklonijima obalnim opasnostima. Korintski zaljev u Grčkoj sa svojim raznolikim obalnim oblicima i tektonskom složenošću čini ovu regiju jedinstvenom u kontekstu procjene ranjivosti obale. U ovom istraživanju primijenjen je integrirani indeks ranjivosti obale (ICVI), koji se sastoji od fizičkih i socioekonomskih parametara, za potencijalni porast razine mora na južnoj obali Korintskog zaljeva (Grčka). Među više različitih metodologija razvijanih posljednjih godina, odabrana su dva matematička pristupa za koje vjerujemo da su najprikladniji za zaštitu ljudskih aktivnosti u našem području istraživanja. Prvi, ICVI_1, temelji se na indeksu obalne ranjivosti (CVI) Thielera i Hammar-Klosea (1999.) s varijablama jednake relativne važnosti, dok drugi, ICVI_2, koristi analitički hijerarhijski proces (AHP) s dodjelom relativnih težinskih vrijednosti za svaki parametar. Parametri su definirani i rangirani u indeks ranjivosti na ljestvici od 1 do 5. Rezultati upućuju na to da oba pristupa prikazuju slične obalne dijelove visoke ili vrlo visoke ranjivosti, ali se razlikuju u distribuciji ekstremnih vrijednosti. ICVI_1 pokazuje da 18,3 % ukupne obale ima vrlo visoku ranjivost (ocjena 5), dok ICVI_2 pokazuje 9,1 %. Obalni dijelovi s najvišim ocjenama ranjivosti uglavnom su zastupljeni u istočnom dijelu proučavane obale s niskim područjima blagog nagiba i koncentrirane ljudske aktivnosti.

Ključne riječi: klimatske promjene, porast razine mora, ranjivost obale, AHP, Korintski zaljev

INTRODUCTION

Long-term sea-level rise is one of the adverse consequences of global warming with immediate and long-term impacts of flooding and erosion on coastal areas (Nicholls Cazenave, 2010). Significant components that contribute to long-term sea-level rise are related to eustatic sea-level changes such as thermal expansion of surface seawater, freshwater mass input from melting continental ice sheets of Greenland and Antarctica, and changes in the shape of the seafloor caused by tectonic activity (Chen et al., 2006; Ramieri et al., 2011; Cazenave, Cozannet, 2013; IPCC, 2013). Moreover, sea-level rise has a different impact on a local scale because sea-level fluctuations are combined with vertical land motion called isostatic adjustment, and therefore sea-level change is observed with respect to a land-based reference called relative sea-level change (Kemp et al., 2011; Mourtzas et al., 2016; Rovere et al., 2016). Research shows that trends of global sea-level rise are related to the acceleration of global sea-level temperatures. More specifically, global sea-level rise was accelerating in the 20th century and beyond with an average of 1.7 mm/yr for the period 1901-2010 and 3.2 mm/yr for 1993-2010 (IPCC, 2013). If the acceleration of mean global temperature continues at the current rate, sea-level temperature is estimated to rise by 1.5 °C between 2030 and 2052, and thus cause further long-term sea-level rise well beyond the next century that may expose small islands, low-lying coastal areas and deltas (IPCC, 2018). In the lowest baseline emissions scenario (RCP2.6) global sea-level is expected to rise by 0.29-0.59 m by the year of 2100 relative to the measures in 1986-2005, and in the highest scenario (RCP8.5) it is expected to rise by 0.51-1.92 m by the year of 2100 (Ipcc, 2019). The process of global warming is expected to intensify coastal storms and extreme sea-levels, implying shoreline retreat and unprecedented flood risk levels by the end of this century (Perch-Nielsen et al., 2008; Vousdoukas et al., 2018; Simeone et al., 2021) with the contributing factors to coastal erosion comprised by astronomical tides, sea surges and wave breaking processes (Merriefield et al., 2013; Hoeke et al., 2015). Vulnerability is a function of both exposure and coping ability of human societies and is therefore both physically and socially dependent (Wu et al., 2002). There are significant trends of population increase in low-lying coastal zones as a result of rapid economic growth (McGranahan et al., 2007; Neumann et al., 2015). If sea-level rise continues with no adaptation measures it is expected to cause loss of land, displacement of coastal population, damage of agricultural production, and disturbance of biodiversity in wetlands, which in turn are expected to generate additional regional economic expenses (Small, Nicholls, 2003; Oliver-Smith, 2009; Hallegate, 2012; You, 2019) reaching 0.3–9.3% of the global gross domestic product by the end of the century (Hinkel et al., 2014). The impact of sea-level rise was measured in monetary terms, not least for the Greek coastlines (Kontogianni et al., 2014). The total financial loss was estimated with long term inundation effects and short-term extreme weather, followed by adaptation measures in response to future sea-level rise.

The assessment of coastal vulnerability to sea-level rise has been applied by using various mathematical approaches (Šimac et al., 2023). The most common method is the Coastal Vulnerability Index (CVI), initially proposed by Gornitz (1991), which was later modified by Thieler and Hammer-Klose (1999), and analyses coastal vulnerability by examining several physical factors influencing coastal erosion. This method was used, not least for the Greek southern coastlines, particularly for the Gulf of Corinth (Karymbalis et al., 2012), but also for the islands of Salamina and Elafonissos (Karymbalis et al., 2014), and the Gulf of Argolís (Gaki-Papanastasiou et al., 2011). However, an integration of socio-economic factors has never been conducted for the Gulf of Corinth and it is highly important to consider it due to the concentration of human activities as well as for the complexity in tectonic and geomorphological processes.

STUDY AREA

The Gulf of Corinth is situated in central Greece and linked to the Gulf of Patras to the west through the narrow and shallow strait of Rio, and to the Gulf of Saronikos to the east by the artificial Corinth Canal. The study area covers the southern path of the Gulf of Corinth, which comprises approximately a 147 km long coastline in the northernmost part of the peninsula of Peloponnese, Greece. The Gulf of Corinth belongs tectonically to the Aegean region, which is one of the most seismically active zones in Europe (Tselentis, Makropoulos, 1986; Bernard et al., 2006; Karymbalis et al., 2012). The submerging African tectonic plate south of Crete collides with the Eurasian one (Makropoulos et al., 2012) resulting in an uplift of the Peloponnese peninsula, which features the 120 km long Corinth Rift, an asymmetric graben structure consisting of active normal faults on each side of the gulf with a W.NW-E.SE orientation, causing the separation of the Peloponnese peninsula from the continental Greece in the NE-SW direction and a speed rate reaching 16 mm/year (Tselentis, Makropoulos, 1986; Armijo et al., 1996; Beckers et al., 2015). The study area consists of the main north dipping active faults of Psathopyrgos, Aigion, Eliki, and Xylokastro (Fig. 1), whose footwall on the southern side of the faults experiences uplift, whereas their hanging walls on the northern side are subsiding (Karymbalis et al., 2012), causing peculiar coastal formations. The western section is characterized by marine cliffs with a high slope, whereas the eastern section by low-lying coastal landscape of gentle slope. The central section is characterised by a transition zone with varied terrain from hilly to flat. In this regard, the relative sea-level of the Gulf of Corinth is dependent on the vertical land movement and the feeding of fluvial deposits to the gulf. Depositional processes are dominated by gravity mass flows such as debris flows and slides mainly caused by earthquakes, but also flood events, causing river-discharging sediment accumulation in the gulf by depositing coarser-grained material along the steeper southern continental shelf and slope (Poulos et al., 1996; Sergiou et al., 2016), developing beaches along the coastal plains and aprons of coastal alluvial fans, featured mainly by coarse sandy to gravels sediments (Karymbalis, 2012).

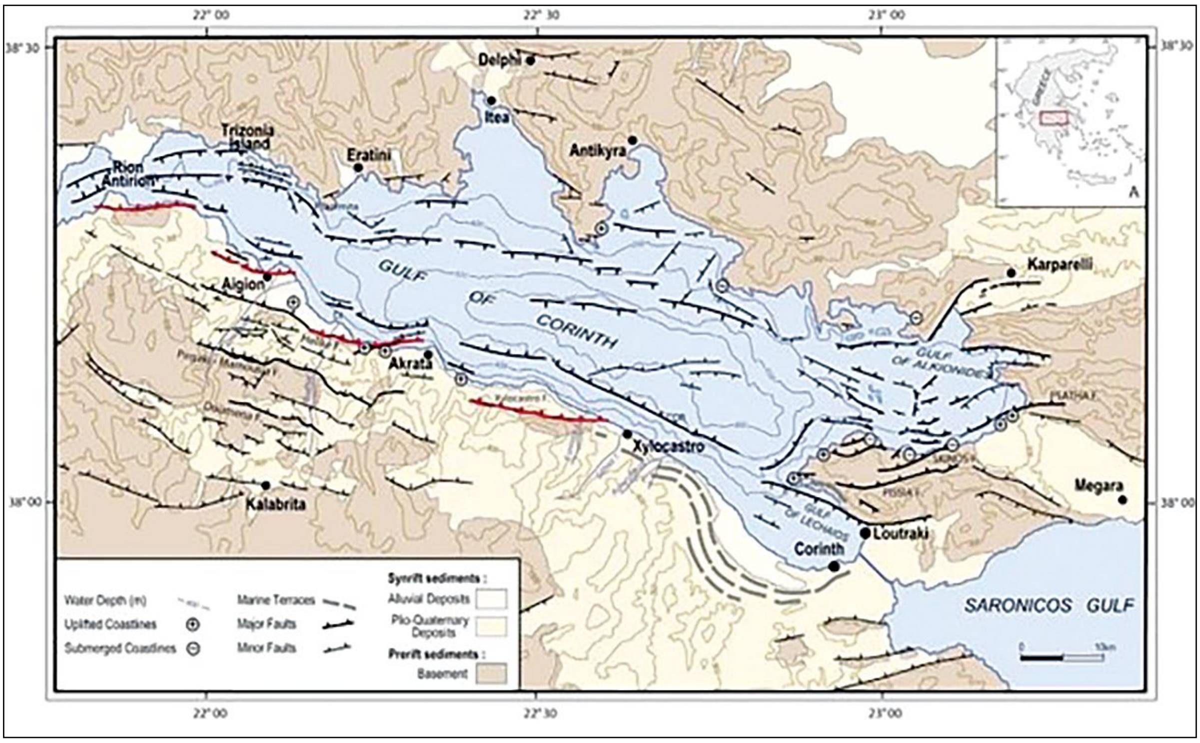

Figure 1 *Structural map of the Gulf of Corinth with depiction of the four most concerned faults in the study area consisting of Psathopyrgos fault, Aigion fault, Eliki fault, and Xylokastro fault (coloured red)*
Source: Moretti et al. (2003)

Table 1 *Significant towns of the study area and their population*

Municipal Unit / Local Community	Corinth	Aegion	Sikyon*	Xylokastro	Rio
Population	30.176	20.664	9.812	5.715	5.252

**Municipality unit of the town Kiato*

Source: URL 1, Mapping Panorama of Greek Census Data 1991-2011

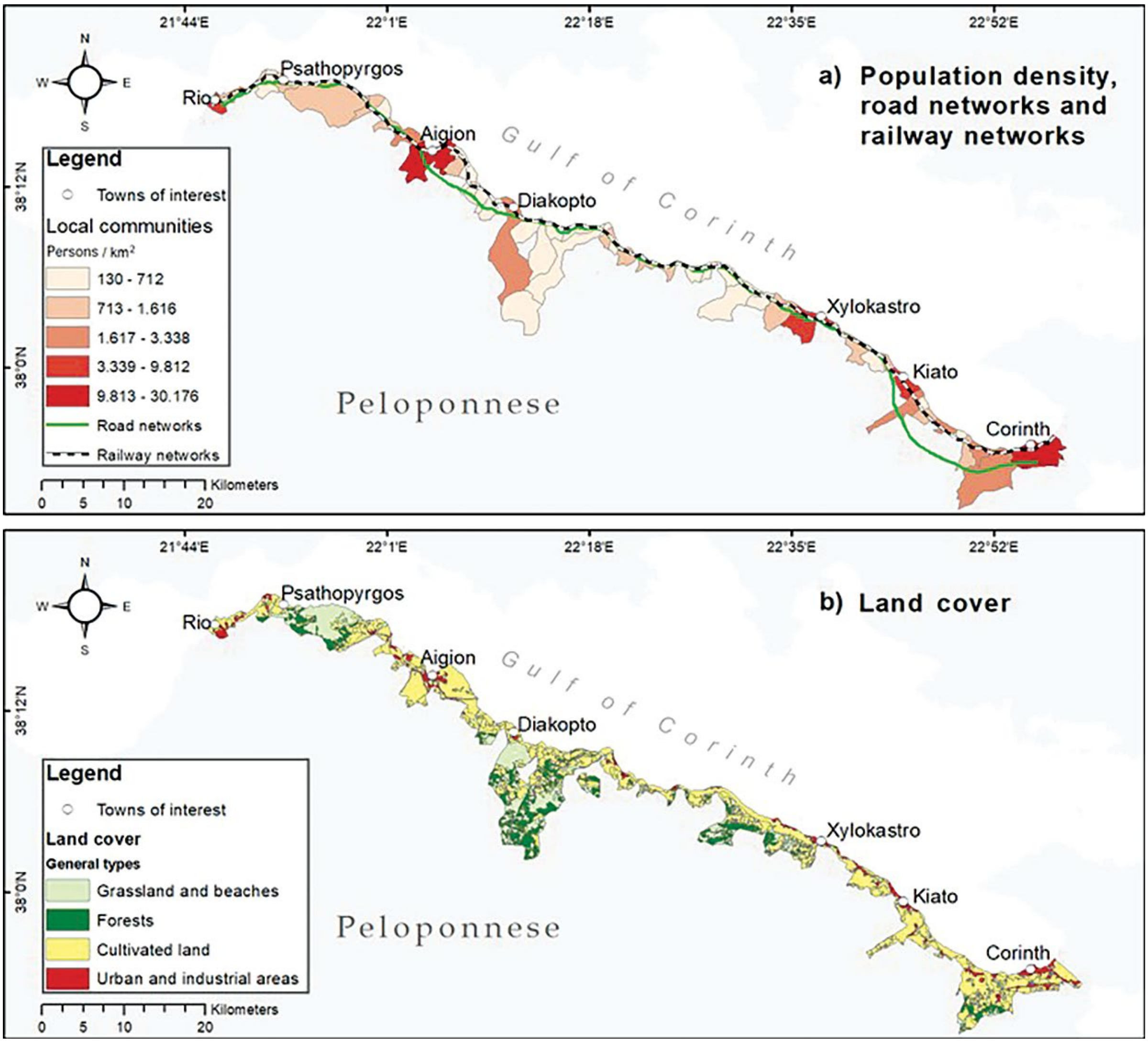

Figure 2 *Maps featuring the areas in local coastal communities a) with road and railway networks, and b) that with land cover*

In terms of climatology, according to the Hellenic National Meteorological Service (URL 2), the region is typical Mediterranean with a mild-cold rainy season from mid-October to late March and a hot dry season which lasts from April to September. The region receives precipitation of 1,300-1,700 mm/year which is considered above the Greek average. The precipitation is characterized by uneven annual distribution where the highest amount is accumulated in the winter season with days of heavy rainfalls during short periods of time. A report by the Bank of Greece (2011) confirms that climate change tends to increase extreme flood events on Greece's extensive coastline caused by intensified short-term precipitation in combination with long-term sea-level rise, and will affect negatively economic activities such as tourism, land use, and transport.

The studied coastline belongs administratively to 52 local communities within the regional units of Corinth and Achaea, and covers an area of 397 km^2. According to the latest available Greek census from 2011, the population reached

119,203 inhabitants (URL 1) with an average of 300 people per square kilometre. The area forms an important cluster of population exceeding the average density of Greece (80 P/km^2), especially during the tourist season. The largest towns are Corinth, Aegion, Kiato, Xylokastro and Rio, all situated on the coastline. The dominant land cover type comprises cultivated vegetation such as vineyards, fruit trees, olive groves and combined crops. One can also find land use types in the urban peripheries comprising minor commercial facilities such as industries and tourist accommodations that offer many forms of alternative tourism. The overwhelming majority of accommodation and tourist facilities are situated on the seafront, serving the tourist high season between May and September. The highway and the railway along the coastline provide a crucial service for passenger transport and international trade between Italy and Greece by linking the city of Athens in the east to the port of Patras in the west.

MATERIALS AND METHODS

This study aims at developing an Integrated Coastal Vulnerability Index (ICVI) for the southern Gulf of Corinth by adding socio-economic parameters to the initial sensitivity assessment conducted by Karymbalis et al. (2012). The physical parameters in this study were those from the commonly used Coastal Vulnerability Index (CVI) proposed by Thieler and Hammer-Klose (1999), which focuses on six physical variables strongly influencing coastal evolution.

$$CVI = \sqrt{\frac{(a * b * c * d * e * f)}{6}}$$

where, a: geomorphology, b: coastal slope, c: relative sea-level rise rate, d: shoreline erosion/accretion rate, e: mean tidal range, and f: mean significant wave height. Socio-economic parameters were added, which include population density, land use/land cover, road networks, and railway networks.

All ten variables were ranked with a scale of vulnerability from 1 to 5, where 1=very low vulnerability, 2=low vulnerability, 3=moderate vulnerability, 4=high vulnerability and 5=very high vulnerability. The ranges for the physical variables were taken from the studies of the Gulf of Argolís (Tragaki et al., 2011) and the Gulf of Corinth (Karymbalis, 2012), which are mentioned as designed for the Greek coastal environments. The values of the socio-economic parameters were set by the authors with relation to their exposure to anticipated sea-level rise, as described further for each parameter.

As for geomorphology, it can be defined as the study of landforms, each one having a degree of resistance to erosion (Bird, 2000) which can be ranked according to the relative strength to marine erosion (Nageswara et al., 2008). They are important to consider in order to manage coastal resources in a sustainable way (Woodrofe, 2002). The predominant landforms identified for the studied shoreline are coarse sandy to gravel beaches and marine cliffs and were retrieved from the Greek Institute of Geology and Mineral Exploration consisting of a geological map at a scale of 1:50,000. The coastal landforms of the studied coastline were classified according to their resistance to coastal erosion. Sandy beaches and deltas were assigned the lowest vulnerability score due to their poor resistance to inundation of sea water, whereas rocky and cliff coasts were given the lowest vulnerability score for their high resistance to sea waves.

Coastal slope is the ratio of altitude to the horizontal distance between any two points on the coast perpendicular to the coastline. Regional coastal slopes indicate the relative vulnerability of inundation and the rate of shoreline retreat (Gaki-Papanastasiou et al., 2011). With that mean, coastal areas with low slope are considered extremely vulnerable because they allow abundant penetration of marine waves over a larger area of the coast, while high slope coastal areas are more resistant to storm surges, therefore exhibiting less vulnerability (Dwarakish et al., 2009; Leaman et al., 2021). The coastal slope for the studied coastline was estimated in percentage. First, a topographic map of northern

Table 2 *Ranges of vulnerability ranking for physical – and socio-economic parameters*

Physical Vulnerability Categories					
Vulnerability score	**Very low (1)**	**Low (2)**	**Moderate (3)**	**High (4)**	**Very high (5)**
Variables					
Geomorphology	Rocky, cliffed coasts	Medium cliffs, indented coasts	Low cliffs, alluvial plains	Cobble beaches, Lagoons	Sandy beaches, deltas
Erosion (-)/accretion (+) rate (m/year)	> (+1.5)	(+1.5)-(+0.5)	(+0.5)-(-0.5)	(-0.5 - (-1.5)	< (-1.5)
Coastal slope (%)	>12	12-9	9-6	6-3	<3
Relative sea level rise (mm/year)	<1.8	1.8-2.5	2.5-3.0	3.0-3.4	>3.4
Mean wave height (m)	<0.3	0.3-0.6	0.6-0.9	0.9-1.2	>1.2
Mean tidal range (m)	<0.2	0.2 -0.4	>0.4-0.6	>0.6-0.8	>0.8
Socio-Economic Vulnerability Categories					
Population density (/km²)	12-116	117-229	230-625	626-1,101	1,102-1,704
Land use/land cover	Water elements	Beaches and grasslands	Forests	Cultivated land	Urban, industrial areas and road network
Road network (distance from coastline in km)	>2.0	1.6-2.0	1.1-1.5	0.5-1.0	<0.5
Railway network (distance from coastline in km)	>2.0	1.6-2.0	1.1-1.5	0.5-1.0	<0.5

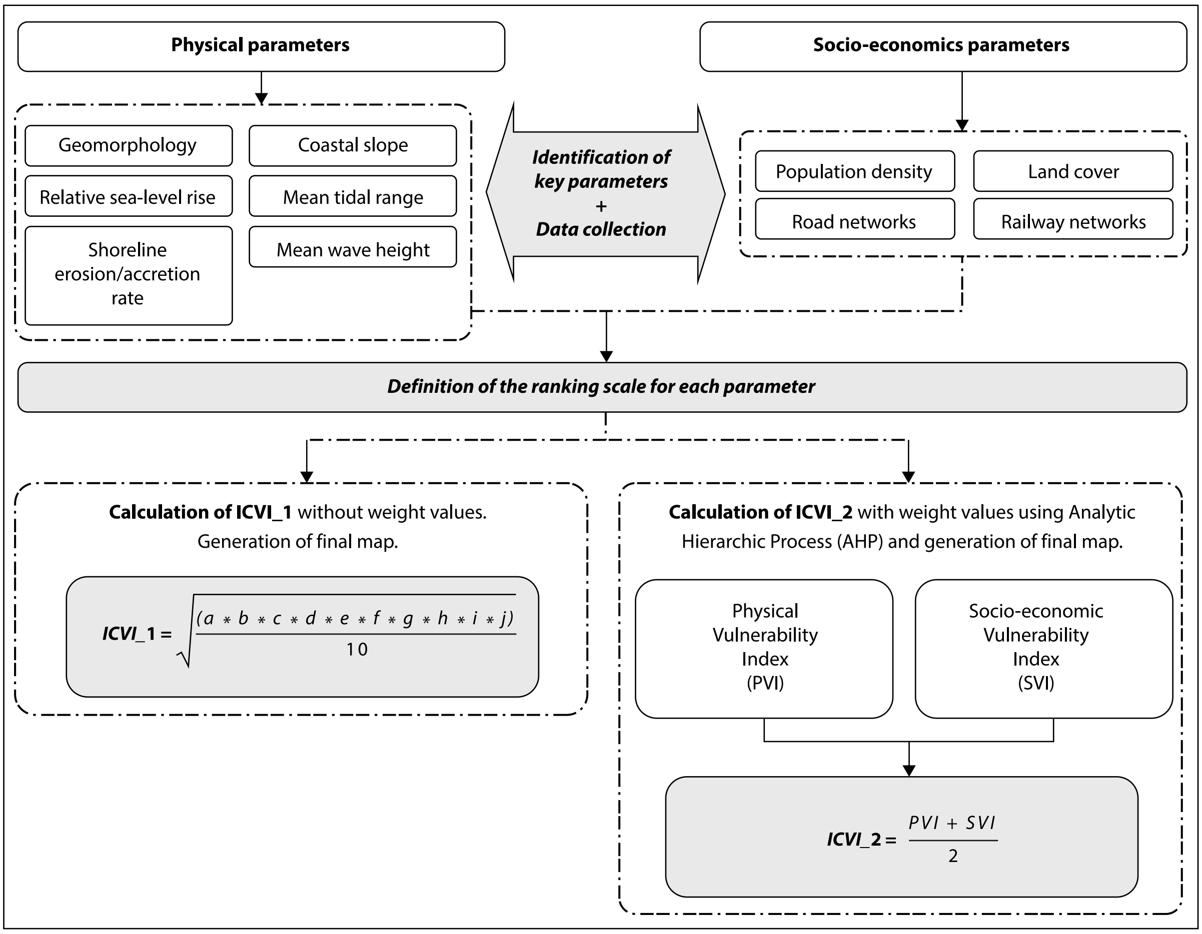

Figure 3 *Flow diagram of the methodology*

Peloponnese was converted to a Digital Elevation Map (DEM) with a focus on elevation of 0-10 m landwards from the coastline. Coastal slope zones were implemented with the ArcGIS software and intersected to the coastline as segments. Slopes of more than 12 degrees represent the highest slope values (Tab. 2) and were assigned very low vulnerability, whereas slopes under 3 degrees represent the lowest slopes and were given a score of very high vulnerability.

Relative sea-level rise in the Gulf of Corinth undergoes a complex physical process due to the interrelation between eustatic sea-level rise, vertical land movements, and the compaction of alluvial sediment deposits. Although several local physical processes have been analysed in the region, there are poor accurate measurements of long term sea-level rise. Consequently, we estimated a given value by Tragaki et al. (2018), which was proposed for the relative sea-level rise in the East Mediterranean of 1.8-2.5 mm/year. Thus, the coastline was given one and only score as of low vulnerability according to the vulnerability ranking scale (Tab. 2).

Shoreline erosion/accretion rates indicate the state of erosion or accretion as the past tendency of a shoreline to retreat or advance due to sea-level rise (Doukakis, 2005; Pantusa et al., 2018; URL 3). In order to estimate the erosion-accretion rate for each section of the studied shoreline, orthophotos were obtained from the Greek Land Registry/Hellenic Cadastre and historical trend of the shoreline was captured by comparing the available years 1945 and 2008 with the latter used as reference layer.

Tide is defined as the change in sea level relative to land and is influenced by the attraction of the moon and the sun to the earth's hydrosphere and has an effect locally with cyclical time varying from region to region (Woodroffe, 2002). When it comes to Greek waters, the astronomical mean tidal range is generally low with the Gulf of Corinth considered as a micro-tidal region. The current mean tidal range for the Gulf of Corinth was estimated from the studies by Karymbalis (2012) and Tsimplis (1994) with a tidal range below 0.15 meters and was given the lowest score of vulnerability.

Waves represent for the most coastlines the dominant source of energy in the nearshore zone and are therefore the driving force behind geomorphologic change (Masselink, 2003) by mobilizing and transporting coastal sediments as a function of wave height (Pendleton et al., 2006). Calculations of coastal vulnerability where mean significant wave height is integrated actually represent the potential for storm erosion (Pantusa, 2018). The Gulf of Corinth is a relatively narrow gulf with its only entrance to open sea through a narrow straight and thus minimizes the energy for the creation of high waves. The mean wave height of the Gulf of Corinth was retrieved from the *Wind and Wave Atlas of the Hellenic Seas* composed by Soukissian et al. (2007), which depicts the annual mean significant wave height ranging from 0 m in the eastern section to 0.3 m in the west. The entire coastline was for that reason given very low vulnerability.

Population density is an important parameter for the assessment of socio-economic vulnerability because it constitutes a crucial factor when estimating population exposure to long term sea-level rise (Tragaki et al., 2018). First, the population data was retrieved from the Hellenic Statistical Authority for each of the 51 local communities that border the studied shoreline. Furthermore, the population density of each local community was calculated by dividing the population with the area of the correspondent local community. Finally, the boundaries of the classes were set with the *Jenks natural breaks* classification method, which indicates a good adaptability and high accuracy on the geographical environment unit division (Chen et al., 2013).

Land use/land cover is another important parameter for assessing coastal vulnerability because land cover indicates the physical land type and helps distinguish built environment from vegetated land. Land use data detects geographically located human activities such as residential areas, commercial use, tourist accommodation and cultivated land. The economic activities and the rapid evolution of the built environment in coastal areas are threatened by a potential sea-level rise (Szlafstein, Sterr, 2007) and for that reason human safety and economic activities have to be prioritized in a coastal vulnerability assessment. Land cover and land use data were retrieved as a shapefile from the electronic data source of *Copernicus Land Monitoring Service* based on the Corine Land Cover 2018, and was limited to the geographical coverage of the local communities. The coastal segments were ranked accordingly by prioritizing human safety and economic activities, giving thus higher vulnerability scores to socio-economic activities and lower vulnerability scores to open wild landscapes.

Road and railway networks were retrieved as a shapefile from the *Ministry of interior of the Hellenic Republic*. As for the road network, the highway was seen as the most in need of protection due to the connectivity between the cities of Patras and Athens, and was for that reason the only used entity of the road network. The highway together with the railway were digitized and buffered separately in a classification of distance from the shoreline, ranging from 0 to 2.0 km where the highest score of vulnerability was determined by the shortest distance from the coastline.

Calculation of the ICVI

There are various methodologies and formulas to calculate the CVI with physical and socio-economic factors. Simac et al. (2023) distinguish three calculation methods: *equal variables*, which is characterized by equal importance of all physical and social variables, *separate variables*, which classifies physical and social vulnerability separately before creating a single vulnerability index, and *causal variables*, which first identifies geographical areas of highest physical vulnerability as a stepping-stone for further vulnerability analysis. Separate variables are utilized in a recent study of the Göksu Delta in southern Turkey (Özyurt, Ergin, 2010) by separating physical parameters and human influence parameters with weighted values. Moreover, a similar method is used for the region of Apulia, Italy, a coastal region which is featured mainly by gentle slope beaches and significant human activity (De Serio et al., 2018). The method uses human parameters named socio-economic and places focus on the exposure of human activities to sea-level rise rather than the influence. Our study area with a high diversity of landforms and a complex tectonic activity poses a challenge to an integrated coastal vulnerability assessment. For that reason, we utilized two calculation methods, one with equal variables and one with separate variables, both previously used for Apulia. The first mathematical approach ICVI_1 was calculated as the square root of the product of 10 variables divided by their total number (10)

$$\boldsymbol{ICVI\_1} = \sqrt{\frac{(a * b * c * d * e * f * g * h * i * j)}{10}}$$

where each parameter a-j is represented by the given score of relative coastal vulnerability for each segment of the coastline. For the physical parameters a: geomorphology, b: coastal slope, c: relative sea-level rise rate, d: shoreline erosion/accretion rate, e: mean tidal range, and f: mean significant wave height. For the socio-economic parameters g: population density, h: land cover/land use, i: road networks, and j: railway networks.

The calculation of ICVI_2 is more complex and constitutes the continuity of the method ICVI_1. In order to calculate ICVI_2 we had to implement the Analytic Hierarchic Process (AHP) (Saaty, 1977; 1990) to obtain the so-called *weight value (Wi)* for each vulnerability score. The AHP is a multi-criteria decision-making tool, which comprises a step by step methodology evaluating all the selected variables to their relative importance by constructing a pairwise comparison matrix with scores from 1 to 9 in the rating scale, where 1 contributes equally to one another and 9 favouring one parameter over another of the highest possible order, always considering the vertical elements in the matrix as a reference. The intensity of importance is as follows: 1=equal, 3=moderate, 5=strong, 7=very strong, 9=extreme. Intermediate values such as 2, 4, 6 and 8 are used when compromise is needed. In the present study the score for each variable was taken from De Serio et al. (2018) who used the pairwise comparison matrix separately for physical parameters and socio-economic parameters (Tab. 3). The weight value for each parame-

Table 3 *Pairwise comparison matrix calculated for all parameters. The relative importance of the physical parameters is set by De Serio et al. (2018)*

	Variables	Geomorphology	Erosion/ accretion rate	Coastal slope	Relative sea level rise	Mean wave height	Mean tidal range
PHYSICAL	Geomorphology	1	5	1/3	6	8	9
	Erosion / accretion rate	1/5	1	1/6	3	4	5
	Coastal slope	3	6	1	4	9	9
	Relative sea level rise	1/6	1/3	1/4	1	3	3
	Mean wave height	1/8	1/4	1/9	1/3	1	2
	Mean tidal range	1/9	1/5	1/9	1/3	1/2	1
	Column Total	**4.603**	**12.783**	**1.972**	**12.999**	**25.500**	**29.000**

	Variables	Population density	Land use	Road network	Railway network
SOCIO-ECONOMIC	Population density	1	4	8	8
	Land use/ Land cover	1/4	1	4	4
	Road networks	1/8	1/4	1	1
	Railway networks	1/8	1/4	1	1
	Column Total	**1.500**	**5.500**	**14.000**	**14.000**

ter was calculated after normalizing the scores of the pairwise comparison matrix as defined by the AHP (Tab. 4).

After having assessed the weight values we verified the consistency of the matrix by checking the consistency ratio (CR) as calculated by the following formula:

$$CR = CI/RI$$

where CI is the consistency ratio index and RI a random index. The consistency index CI is expressed as:

$$CI = \frac{(\lambda_{max} - n)}{(n - 1)}$$

where λ_{max} is the principal eigenvalue of the matrix and n is the order of the matrix.

If CR <0.10 the matrix is consistent.

After ensuring that CR<0.10, the Physical Vulnerability Index (PVI) and the Socio-economic Vulnerability Index (SVI) were calculated separately as shown below.

The calculation of PVI and SVI were based on the Weighted Linear Combination method and comprises the sum (Σ) of weighted rating scores:

$$V = \sum_{i=1}^{n} Wi * Xi$$

where V stands for the vulnerability degree, n is the number of total factors, Wi is the weight of the corresponding factor i, and Xi is the rating of the factor i. The development of the mathematical formula for the PVI and SVI is shown below.

$$PVI = (W_1 * X_1) + (W_2 * X_2) + (W_3 * X_3) + (W_4 * X_4) + (W_5 * X_5) + (W_6 * X_6)$$

$$SVI = (W_7 * X_7) + (W_8 * X_8) + (W_9 * X_9) + (W_{10} * X_{10})$$

The final calculation of ICVI_2 was completed by deriving the average value of the PVI and SVI.

$$\textbf{\textit{ICVI\_2}} = \frac{PVI + SVI}{2}$$

The coastal vulnerability mapping was computed in the ArcGIS environment by initial-

Table 4 *Normalized scores of the pairwise comparison matrix and the calculated weight value (W) for each variable*

PHYSICAL	Variables	Geomorphology	Erosion/ accretion rate	Coastal slope	Relative sea level rise	Mean wave height	Mean tidal Range	W
	Geomor-phology	0.217	0.391	0.169	0.500	0.314	0.310	**0.317**
	Erosion/ accretion rate	0.043	0.078	0.085	0.028	0.157	0.172	**0.094**
	Coastal slope	0.652	0.469	0.507	0.333	0.353	0.310	**0.437**
	Relative sea level rise	0.036	0.026	0.127	0.083	0.118	0.103	**0.082**
	Mean wave height	0.027	0.020	0.056	0.028	0.039	0.069	**0.040**
	Mean tidal range	0.024	0.016	0.056	0.028	0.020	0.034	**0.030**

SOCIO-ECONOMIC	Variables	Population density	Land use/ Land cover	Road networks	Railway networks	W
	Population density	0.667	0.727	0.571	0.571	**0.634**
	Land use/ land cover	0.167	0.182	0.286	0.286	**0.230**
	Road net-works	0.083	0.045	0.071	0.071	**0.068**
	Railway networks	0.083	0.045	0.071	0.071	**0.068**

ly segmenting the coastline separately for each variable according to the vulnerability score (1-5) to coastal inundation. Each coastal segment was then calculated by utilizing the two defined mathematical approaches separately. In order to achieve the relative ICVI for the study area, the outcome score of each coastal segment was classified with the Jenks classification method.

RESULTS AND DISCUSSION

The studied coastline of the southern Gulf of Corinth was found to feature geographical sections of various levels of relative vulnerability, from very low to very high. As regards to physical parameters, the coastline with the largest share of high and very high vulnerability relates to the coastal slope and geomorphology. The high value of the coastal slope stretches from Aigion to Corinth (Fig. 4), whereas the high value of geomorphology covers the whole coastline. Erosion/accretion rate on the other hand features mostly high vulnerability rate with a notable small section of very high vulnerability rate west of Xylokastro as a result of coastal erosion since 1945. Relative sea-level rise, mean wave height and mean tidal range cover very low vulnerability. As for socio-economic parameters, the highest coverage of a very high vulnerability score is featured by road and railway networks, whereas the population density and land cover/ land use show a smaller share. The coastal area between Corinth and Kiato is a gently sloping area with a significant proportion of the built environment consisting of housing, factories and compact road networks. The road networks are characterized as having very low vulnerability in the easternmost section due to the significant distance of the highway to the coastline. Physical parameters applied with the AHP method as shown in Fig. 5, constitute 13.7% as

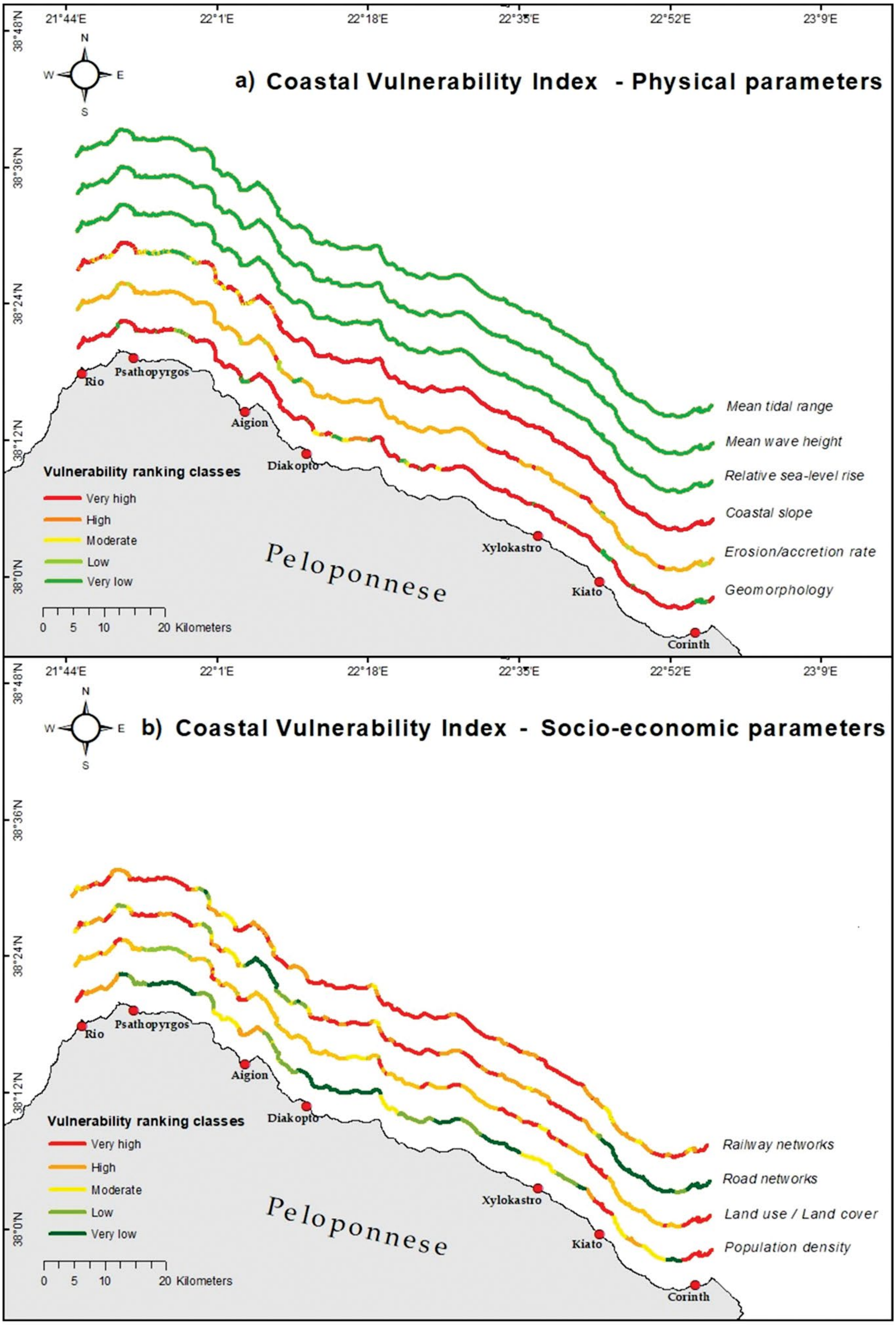

Figure 4 *Maps depicting coastal vulnerability classification of the southern Gulf of Corinth with a) physical variables and b) socio-economic variables*

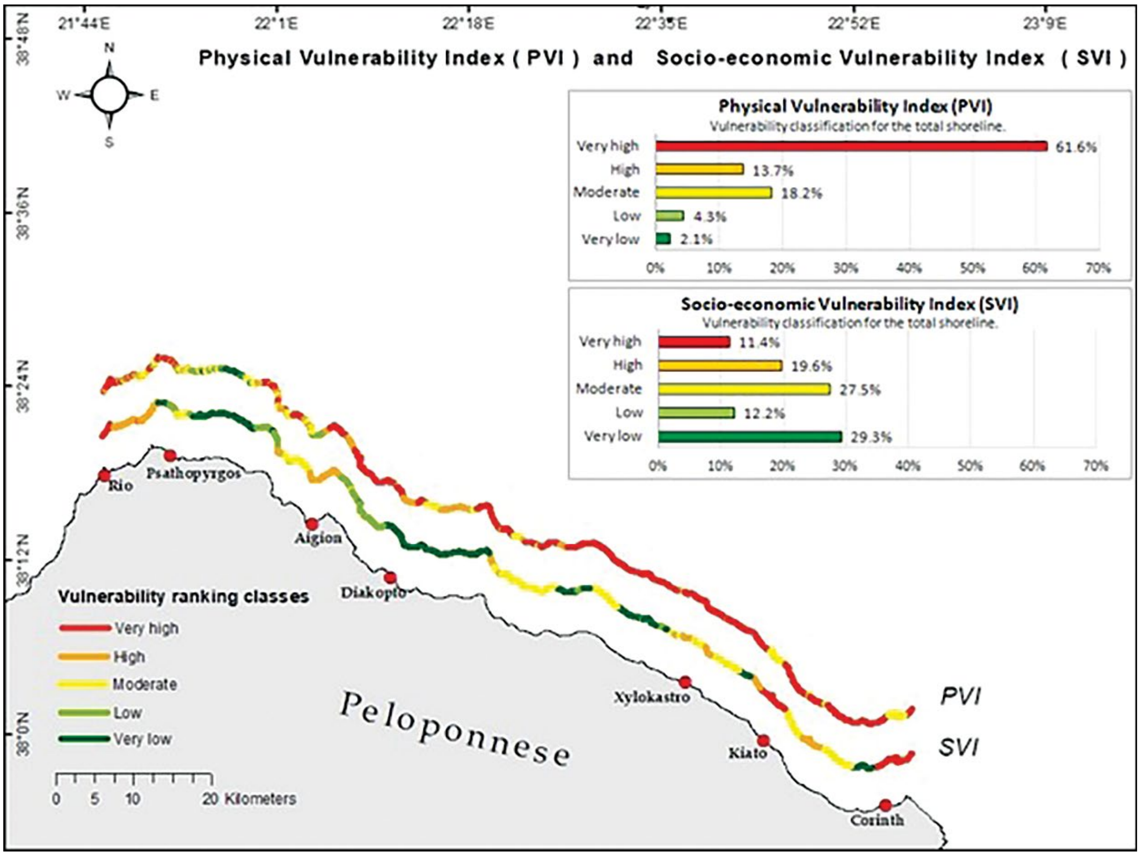

Figure 5 *Map depicting the vulnerability classification of the Physical Vulnerability Index (PVI) and the Socio-Economic Vulnerability Index (SVI)*

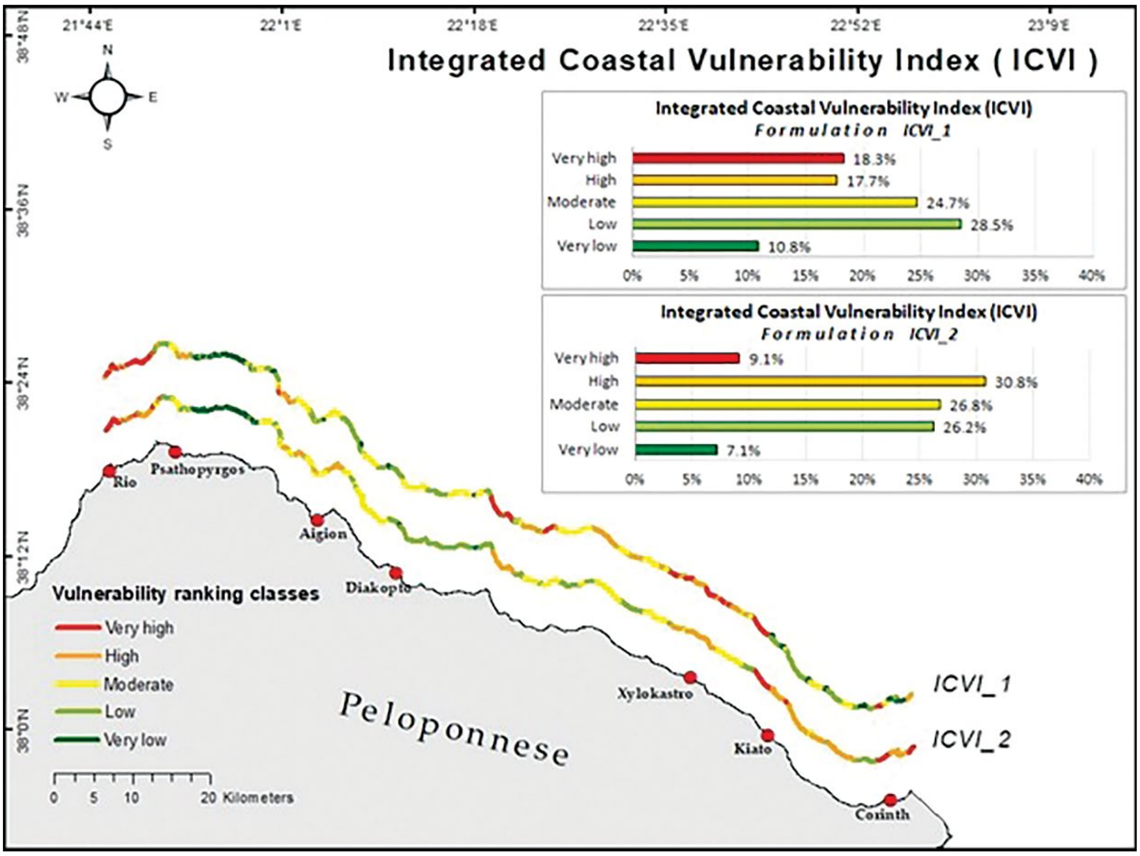

Figure 6 *Final map of the Integrated Coastal Vulnerability Index to sea-level rise for the southern Gulf of Corinth, with ICVI_1 corresponding to the first mathematical approach, and the ICVI_2 to the second approach with the utilized AHP-method*

of high vulnerability and 61.6% as of very high vulnerability, which together comprise a rate of 75.3% high or very high vulnerability, mainly distributed in the eastern coastline with plain morphological features. The socio-economic entity on the other hand comprises its high values of vulnerability in a lower degree with 16.7% of high vulnerability and 11.4% of very high vulnerability.

The results of the two mathematical approaches (ICVI_1 and ICVI_2), consist of six physical parameters and four socio-economic parameters. In Fig. 6, the first approach (ICVI_1) shows that 18.3% of the studied coastline is characterized as having a very high vulnerability, while 10.8% as having a very low vulnerability. In the second approach (ICVI_2) very high and very low vulnerability stand for 9.1% and 7.1% respectively. In general, both methods show very high to high vulnerability mainly in the eastern section of the coastline, whilst in the central and western section the aforementioned values are presented in a shorter overall length. The values of high and very high vulnerability are depicted in the most densely populated settlements, which are Corinth, Kiato and Xylokastro in the eastern section, and Rio in the western one. The lowest vulnerability (very low score) is depicted in Psathopyrgos due to the occurrence of marine cliffs. To sum up, the results depict a relatively extensive coastal segment of high or very high vulnerability to a potential sea-level rise.

CONCLUSIONS

The present study utilized two mathematical approaches to quantify the coastal vulnerability to a potential sea-level rise of the southern Gulf of Corinth by accounting socio-economic and physical parameters. Same coastal sections are highlighted as more vulnerable than others (high and very high) in both approaches, mostly the eastern coast of the southern Gulf of Corinth (between the settlements of Corinth and Kiato) featured by flat coastal areas, which host important transport network and urban hubs, such as Rio, Xylokastro and Aigion. As such, the two methods seem to respond to the imprint of reality in a coastal region with a high variety of landforms. The implementation of the two mathematical approaches revealed the complexity of achieving a true and fair assessment of coastal vulnerability when integrating human activities to natural processes. The results of the two approaches show differences in the extreme vulnerability values, where the first approach (ICVI_1) expresses a higher proportion of extreme values compared to the second (ICVI_2). It can be attributed to the lower given importance of the socio-economic attributes in the ICVI_1 as well as the added weights to each variable in the ICVI_2. To this meaning, it is fundamental that each parameter is assigned the correct relative importance in order for the results to reflect an accurate vulnerability of the studied region. Equally important is to extract accurate data from reliable sources that represent the studied region, as outdated information or small discrepancies in quantitative data may alter the results after the assignments of weights. A high number of included parameters are also generators for altering the results because the particular influence of each parameter decreases. By saying this, each parameter contributes to vulnerability with unequal importance in nature and therefore a weighted procedure is highly recommended, especially when incorporating socio-economic parameters, which are considered human induced attributes. The utilized approaches in this study are recommended to be applied in similar environments by assigning weights of relative importance according to the priorities. Both constitute a first large-scale assessment in order to catch the most vulnerable coastal regions that need to be protected from future flooding and erosion caused by future sea-level rise or severe storm surge events.

SOURCES AND BIBLIOGRAPHY

Armijo, R., Meyer, B., King, G. C. P., Rigo, A., Papanastassiou, D. (1996): Quaternary evolution of the Corinth Rift and its implications for the Late Cenozoic evolution of the Aegean, *Geophysical Journal International*, Oxford University Press, 126 (1), 11-53, DOI: 10.1111/j.1365-246X.1996.tb05264.x.

Bank of Greece (2011): *The environmental, economic and social impacts of climate change in Greece*, Bank of Greece, Athens, Greece, 2011.

Beckers, A., Hubert-Ferrari, A., Beck, C., Bodeux, S., Tripsanas, E., Sakellariou, D., De Batist, M. (2015): Active faulting at the western tip of the Gulf of Corinth, Greece, from high-resolution seismic data, *Marine Geology*, 360, 55-69, DOI: 10.1016/j.margeo.2014.12.003

Bernard, P., Lyon-Caen H., Briole P., Deschamps, A., Boudin F., Makropoulos, K., Papadimitriou, P., Lemeille, F., Patau, G., Billiris, H., Paradissis, D., Papazissi, K., Castarede, H., Charade, O., Nercessian, A., Avallone, A., Pacchiani, F., Zahradnik, J., Sacks, S., Linde, A. (2006): Seismicity, deformation and seismic hazard in the western rift of Corinth: New insights from the Corinth Rift Laboratory (CRL), *Tectonophysics*, 426 (1-2), 7-30, DOI: 10.1016/j.tecto.2006.02.012.

Bird, E. C. F. (2000): *Coastal geomorphology: an introduction*, Publisher "J.Wiley & Sons", 2nd ed., Chichester, England, pp. 436.

Cazenave, A., Le Cozannet, G. (2013): Sea level rise and its coastal impacts, *AGU*, 2 (2), 15-34, DOI: 10.1002/2013EF000188.

Chen, J., Yang, S., Li, H., Zhang, B., Lv, J. (2013): Research on geographical environment unit division based on the method of natural breaks (Jenks), *International Archives of the Photogrammetry, Remote Sensing and Spatial Information Sciences*, XL-4/W3, 47–50, DOI: 10.5194/isprsarchives-XL-4-W3-47-2013.

Chen, J. L., Wilson, C. R., Tapley, B. D. (2006): Satellite gravity measurements confirm accelerated melting of Greenland ice sheet, *Science*, 313 (5795), 1958-1960, DOI: 10.1126/science.1129007.

De Serio, f., Armenio, E., Mossa, M., Petrillo, A. F. (2018): How to Define Priorities in Coastal Vulnerability Assessment, *Geosciences*, 8 (11), 415, DOI: 10.3390/geosciences8110415.

Doukakis, E. (2005): Coastal Vulnerability and Risk Parameters, *European Water,* 11 (12), 3-7.

Dwarakish, G. S., Vinary, S. A., Natesan, U., Asano, T., Kakinuma, T., Venkataramana, K., Jagedeesha, B., Badita, M. K. (2009): Coastal vulnerability assessment of the future sea-level rise in Udupi coastal zone of Karnataka state, west coast of India, *Ocean & Coastal Management*, 52, 467-478, DOI: 10.1016/j.ocecoman.2009.07.007.

Gaki-Papanastassiou, K., Karymbalis, E., Poulos, S., Seni, A., Zouva, C. (2011): Coastal vulnerability assessment to sea-level rise based on geomorphological and oceanographical parameters: The case of Argolikos Gulf, Peloponnese, Greece, *Hellenic Journal of Geosciences*, 45, 109-122.

Gornitz, V. (1991): Global coastal hazards from future sea level rise. *Palaeogeography, Palaeoclimatology, Palaeoecology*, 89, 379-398, DOI: 10.1016/0031-0182(91)90173-O.

Hallegatte, S. (2012): A Framework to Investigate the Economic Growth Impact of Sea Level Rise. *Environmental Research Letters,* 7 (1), 1–7, DOI: 10.1088/1748-9326/7/1/015604.

Hinkel, J., Lincke, D., Vafeidis, A. T., Perrette, M., Nicholls, R. J., Tol, R. S. J., Marxeion, B., Fettweis, X., Ionescu, C., Levermann, A. (2014): Coastal flood damage and adaptation costs under 21st century sea-level rise. *Proceedings of the National Academy of Sciences,* 111 (9), 3292–3297, DOI: 10.1073/pnas.1222469111.

Hoeke, R., Mcinnes, K., O'grady, J. (2015): Wind and Wave Setup Contributions to Extreme Sea Levels at a Tropical High Island: A Stochastic Cyclone Simulation Study for Apia, Samoa, *Journal of Marine Science and Engineering*, 3 (3), 1117–1135, DOI: 10.3390/jmse3031117.

IPCC (2013): *Climate Change 2013: The Physical Science Basis. Contribution of Working Group I to the Fifth Assessment Report of the Intergovernmental Panel on Climate Change*, Cambridge University Press, Cambridge, United Kingdom and New York, NY, USA, 2013, available at: https://www.ipcc.ch/report/ar5/wg1/

IPCC (2018): *Global warming of 1.5°C. An IPCC Special Report on the impacts of global warming of 1.5°C above pre-industrial levels and related global greenhouse gas emission pathways, in the context of strengthening the global response to the threat of climate change, sustainable development, and efforts to eradicate poverty*, World Meteorological Organization, Geneva, Switzerland, 2018, 32, available at: https://www.ipcc.ch/sr15/

IPCC (2019): *IPCC Special Report on the Ocean and Cryosphere in a Changing Climate*. In press.

Karymbalis, E., Chalkias C., Chalkias, G., Grigoropoulou, E., Manthos, G., Ferentinou, M. (2012): Assessment of the sensitivity of the Southern Coast of the Gulf of Corinth (Peloponnese, Greece) to Sea-level Rise, *Central European Journal of Geosciences*, 4 (4), 561-577, DOI: 10.2478/s13533-012-0101-3.

Karymbalis, E., Chalkias, C., Ferentinou, M., Chalkias, G., magklara, M. (2014): Assessment of the Sensitivity of Salamina (Saronic Gulf) and Elafonissos (Lakonic Gulf) islands to Sea-level Rise. *Journal of Coastal Research,* 70, 378–384, DOI: 10.2112/SI70-064.1

Kemp, A. C., Horton, B. P., Donnelly, J. P., Mann, M. E., Vermeer, M., Rahmstorf, S. (2011): Climate related sea-level variations over the past two millennia, *Proceedings of the National Academy of Sciences of the United States of America*, 108 (27), 11017-11022, DOI: 10.1073/pnas.1015619108

Kontogianni, A., Tourkolias, C. H., Damigos, D., Skourtos, M. (2014): Assessing sea level rise costs and adaptation benefits under uncertainty in Greece, *Environmental Science & Policy,* 37, 61–78, DOI: 10.1016/j.envsci.2013.08.006

Leaman, C. K., Harley, M. D., Splinter, K. D., Thran, M. C., Kinsela, M. A., Turner, I. L. (2021): A storm hazard matrix combining coastal flooding and beach erosion, *Coastal Engineering,* 170, 104001, DOI: 10.1016/j.coastaleng.2021.104001.

Makropoulos, K., Kaviris, G., Kouskouna, V. (2012): An updated and extended earthquake catalogue for Greece and adjacent areas since 1900, *Natural Hazards and Earth System Sciences*, 12, 1425-1430, DOI: 10.5194/nhess-12-1425-2012.

Masselink, G. (2003): *Introduction to coastal processes and geomorphology*, Oxford University Press, London.

Mcgranahan, G., Balk, D., Anderson, B. (2007): The rising tide: assessing the risks of climate change and human settlements in low elevation coastal zones. *Environment and Urbanization,* 19 (1), 17–37, DOI: 10.1177/0956247807076960.

Merrifield, M. A., Genz, A. S., Kontoes, C. P., marra, J. J. (2013): Annual maximum water levels from tide gauges: Contributing factors and geographic patterns. *Journal of Geophysical Research: Oceans,* 118 (5), 2535-2546, DOI: 10.1002/jgrc.20173.

Moretti, I., Sakellariou, D., Lykousis, V., Micarelli, L. (2003): The Gulf of Corinth: an active half graben?, *Journal of Geodynamics*, 36 (1), 323-340, DOI: 10.1016/S0264-3707(03)00053-X.

Mourtzas, N., Kolaiti, E., Anzidei, M. (2016): Vertical land movements and sea level changes along the coast of Crete (Greece) since Late Holocene, *Quaternary International,* 401, 43–70, DOI:10.1016/j.quaint.2015.08.008.

Nageswara Rao, K., Subraelu, P., Venkateswara Rao, T., Hema Malini, B., Ratheesh, R., Bhattacharya, S., Rajawat, A. S. (2008): Sea-level rise and coastal vulnerability: an assessment of Andhra Pradesh coast, India through remote sensing and GIS, *Journal of Coastal Conservation*, 12 (4), 195–207, DOI: 10.1007/s11852-009-0042-2.

Neumann, B., Vafeidis, A. T., Zimmermann, J., Nicholls, R. J. (2015): Future coastal population growth and exposure to sea-level rise and coastal flooding - A global assessment, *PLoS ONE*, 10 (3), e0118571, DOI:10.1371/journal.pone.0118571.

Nicholls, R. J., Cazenave, A. (2010): Sea-level rise and its impact on coastal zones, *Science*, 328 (5985), 1517-1520. DOI: 10.1126/science.1185782.

Oliver-Smith, a. (2009): Sea Level Rise and the Vulnerability of Coastal Peoples: Responding to the Local Challenges of Global Climate Change in the 21st Century, *United Nations University – Institute for Environment and Human Security*, No.7., available at: https://www.unisdr.org/files/14028_4097.pdf

Özyurt, G., Ergin, A. (2010): Improving Coastal Vulnerability Assessments to Sea-Level Rise: A New Indicator-Based Methodology for Decision Makers, *Journal of Coastal Research,* 26 (2), 265–273, DOI: 10.2112/08-1055.1.

Pantusa, D., D'alessandro, F., Riefolo, L., Principato, F., Tomasicchio, R. G. (2018): Application of a Coastal Vulnerability Index. A Case Study along the Apulian Coastline, *Water*, 10 (9), 1218, DOI: 10.3390/w10091218.

Pendleton, E. A., Thieler, E. R., Williams, S. J. (2006): Coastal vulnerability assessment of Glacier Bay National Park to sea-level rise: *U.S. Geological Survey Open-File Report*, 2005-1247, available at: pubs.usgs.gov/of/2005/1247

Perch-Nielsen, L. S., B. Bättig, M., Imboden, D. (2008): Exploring the link between climate change and migration, *Climatic Change,* 91 (3-4), 375-393, DOI:10.1007/s10584-008-9416-y.

Poulos, S. E., Collins, M. B., Pattiaratchi, C., Cramp, A., Gull, W., Tsimplis, M., Papatheodorou, G. (1996): Oceanography and sedimentation in the semi-enclosed, deep-water Gulf of Corinth (Greece). *Marine Geology,* 134 (3-4), 213–235, DOI: 10.1016/0025-3227(96)00028-x.

Ramieri, E., Hartley, A., Barbanti, A., Santos, F. D., Gomes, A., Laihonen, P., Marinova, N., Santini, m. (2011): Methods for assessing coastal vulnerability to climate change, ETC/CCA Technical Paper, *EEA - European Environment Agency*, Bologna.

Rovere, A., Stocchi, P., Vacchi, M. (2016): Eustatic and Relative Sea Level Changes, *Current Climate Change Reports,* 2 (4), 221–231, DOI: 10.1007/s40641-016-0045-7.

Saaty, T. L. (1977): A scaling method for priorities in hierarchical structures, *Journal of Mathematical Psychology*, 15 (3), 234–281, DOI: 10.1016/0022-2496(77)90033-5.

Saaty, T. L. (1990): How to make a decision: The analytic hierarchy process, *European Journal of Operational Research,* 48 (1), 9–26, DOI: 10.1016/0377-2217(90)90057-I.

Sergiou, S., Beckers, A., Geraga, M., Papatheodorou, G., Iliopoulos, I., Papaefthymiou, H. (2016): Recent sedimentary process in the western gulf of Corinth, Greece: Seismic and aseismic turbitides, *Bulletin of the Geological Society of Greece*, 50 (1), 383–391, DOI: 10.12681/bgsg.11739.

Šimac, Z., Lončar, N., Faivre, S. (2023): Overview of Coastal Vulnerability Indices with Reference to Physical Characteristics of the Croatian Coast of Istria, *Hydrology*, 10 (1), 14, DOI: 10.3390/hydrology10010014.

Simeone, S., Palombo, L., Molinaroli, E., Brambill, W., Conforti, A., De Falco, G. (2021): Shoreline Response to Wave Forcing and Sea Level Rise along a Geomorphological Complex Coastline (Western Sardinia, Mediterranean Sea), *Applied Sciences*, 11 (9), 4009, DOI: 10.3390/ app11094009.

Small, C., Nicholls, R. J. (2003): A global analysis of human settlement in coastal zones, *Journal of Coastal Research*, West Palm Beach, Florida, 19 (3), 584-599.

Soukissian, T., Hatzinaki, M., Korres, G., Papadopoulos, A., Kallos, G., Anadranistakis, E. (2007): Wind and Wave Atlas of the Hellenic Seas, *Hellenic Centre for Marine Research,* pp. 300.

Szlafsztein, C., Sterr, H. (2007): A GIS-based vulnerability assessment of coastal natural hazards, state of Pará, Brazil, *Journal of Coastal Conservation*, 11, 53–66, DOI: 10.1007/s11852-007-0003-6.

Thieler, E. R., Hammar-Klose, E. S. (1999): National Assessment of Coastal Vulnerability to Sea-Level Rise: Preliminary Results for the U.S. Atlantic Coast, *U.S. Geological Survey Open File Report*, 99-593.

Tragaki, A., Gallousi, C., Karymbalis, E. (2018): Coastal Hazard Vulnerability Assessment Based on Geomorphic, Oceanographic and Demographic Parameters: The Case of the Peloponnese (Southern Greece), *Land*, 7 (2), 56, DOI: 10.3390/land7020056.

Tselentis, G. A., Makropoulos, K. (1986): Rates of crustal deformation in the Gulf of Corinth [central Greece] as determined from seismicity, *Tectonophysics*, 124 (1-2), 55–66, DOI: 10.1016/0040-1951(86)90137-X.

Tsimplis, M. N. (1994): Tidal oscillations in the Aegean and Ionian Seas, *Estuarine, Coastal and Shelf Science,* 39, 201–208.

URL 1, *Mapping Panorama of Greek Census Data 1991-2011,* ELSTAT, http://panorama.statistics.gr, 25.9.2021.

URL 2, *Hellenic National Meteorological Service – HNMS*, www.emy.gr/emy/en/, 19. 9. 2021

URL 3, *National Coastal Vulnerability Assessment and Designing of Integrated Coastal Management and Adaptation Strategic Plan for Timor-Leste, Coastal Vulnerability Assessment Report*, United Nations Development Program, 2018, www.undp.org/publications, 20.09.2021

Vousdoukas, M. I., Mentashi, L., Voukouvalas, E., Verlaan, M., Jevrejeva, S., Jackson, L. P., Feyen, L. (2018): Global probabilistic projections of extreme sea levels show intensification of coastal flood hazard, *Nature Communications,* 9 (1), DOI: 10.1038/s41467-018-04692-w.

Woodroffe, C. D. (2002): *Coasts: form, process and evolution*, Cambridge University Press, New York.

Wu S., Yarnal B., Fisher A., (2002): Vulnerability of coastal communities to sea-level rise: a case study of Cape May County, New Jersey, USA, *Climate Research*, 22, 255-270, DOI: 10.3354/cr022255.

You, Z. J. (2019): Tropical Cyclone-Induced Hazards Caused by Storm Surges and Large Waves on the Coast of China, *Geosciences,* 9 (3), 131, DOI:10.3390/geosciences9030131.